Halogen bonding properties of 4-iodopyrazole and 4-bromopyrazole explored by rotational spectroscopy and ab initio calculations

Graham. A. Cooper, Chris Medcraft, Josh D. Littlefair, Thomas J. Penfold, and Nicholas R. Walker

Citation: J. Chem. Phys. **147**, 214303 (2017); doi: 10.1063/1.5002662
View online: https://doi.org/10.1063/1.5002662
View Table of Contents: http://aip.scitation.org/toc/jcp/147/21
Published by the American Institute of Physics

Halogen bonding properties of 4-iodopyrazole and 4-bromopyrazole explored by rotational spectroscopy and *ab initio* calculations

Graham. A. Cooper,[a] Chris Medcraft,[b] Josh D. Littlefair, Thomas J. Penfold, and Nicholas R. Walker[c]
Chemistry–School of Natural and Environmental Sciences, Newcastle University, Bedson Building, Newcastle-upon-Tyne NE1 7RU, United Kingdom

(Received 31 August 2017; accepted 16 October 2017; published online 1 December 2017)

The combination of halogen- and hydrogen-bonding capabilities possessed by 4-bromopyrazole and 4-iodopyrazole has led to them being described as "magic bullets" for biochemical structure determination. Laser vaporisation was used to introduce each of these 4-halopyrazoles into an argon gas sample undergoing supersonic expansion prior to the recording of the rotational spectra of these molecules by chirped-pulse Fourier transform microwave spectroscopy. Data were obtained for four isotopologues of 4-bromopyrazole and two isotopologues of 4-iodopyrazole. Isotopic substitutions were achieved at the hydrogens attached to the pyrrolic nitrogen atoms of both 4-halopyrazoles and at the bromine atom of 4-bromopyrazole. The experimentally determined nuclear quadrupole coupling constants, $\chi_{aa}(\mathrm{X})$ and $\chi_{bb}(\mathrm{X}) - \chi_{cc}(\mathrm{X})$, of the halogen atoms (where X is the halogen atom) of each molecule are compared with the results of the *ab initio* calculations and those for a range of other halogen-containing molecules. It is concluded that each of 4-bromopyrazole and 4-iodopyrazole will form halogen bonds that are broadly comparable in strength to those formed by CH_3X and CF_3X. *Published by AIP Publishing.* https://doi.org/10.1063/1.5002662

I. INTRODUCTION

Compounds containing the pyrazole ring motif have a wide range of applications in medicinal chemistry and other areas such as catalysis.[1] Pyrazole is known to inhibit the action of alcohol dehydrogenase (ADH),[2] while 4-methylpyrazole (also known as fomepizole) effectively blocks the metabolism of methanol by ADH and is currently the recommended antidote for methanol poisoning.[3,4] 4-Bromopyrazole and 4-iodopyrazole retain an ability to function as inhibitors of ADH action[5,6] but are potentially of much broader interest. The combination of halogen- and hydrogen-bonding capabilities possessed by each of these halopyrazoles has led to them being labeled as "magic bullets" for biochemical structure determination.[7]

Rotational spectroscopy can be used to provide information about the geometric and electronic structures of molecules. Microwave spectra have previously been reported for the isolated pyrazole molecule in the gas-phase[8–14] and also for derivatives and complexes.[15–17] This report describes the pure rotational spectra of 4-bromo- and 4-iodopyrazole, which have been recorded for the first time. The data are analyzed and found to be consistent with the planar geometries expected for these molecules. Hyperfine structures in microwave spectra provide information about the occupation of molecular orbitals close to quadrupolar nuclei[18,19] and can inform the understanding of the nature of intermolecular interactions such as halogen bonding, which rely strongly on the form of the electron distribution around the nucleus.[20–22] During this work, it will be shown that the hyperfine structure in the microwave spectra of 4-bromo- and 4-iodopyrazole provides an important perspective on charge distributions within these molecules.[18] The data are interpreted with reference to the ability of the 4-halopyrazoles to form strong intermolecular, halogen bonding interactions. The results provide a novel perspective from which to examine the observations of Bauman *et al.* concerning the usefulness of these molecules for protein crystallography.[7]

II. EXPERIMENTAL

Each molecule was transferred into the gas phase by laser ablation of a solid rod containing the appropriate 4-halopyrazole in a copper matrix. Solid rod targets of 5 mm in diameter were prepared (respectively, for each of 4-bromopyrazole and 4-iodopyrazole) by compressing an equimolar mixture of the 4-halopyrazole (Sigma-Aldrich, 99%) with copper powder (Sigma-Aldrich, <75 μm, 99%). Laser ablation of the solid rod target was achieved using the focused second harmonic output of an Nd:YAG laser (532 nm, 20 mJ/pulse, 10 ns pulses). A small quantity of the laser-vaporised 4-halopyrazole was thus entrained in a flow of argon gas (BOC Pureshield Argon) undergoing supersonic expansion into the CP-FTMW (chirped-pulse Fourier transform microwave spectrometer) spectrometer. The argon carrier gas was introduced from a cylinder held at a backing pressure of 7 bar via a pulsed valve. The experiment employed a 2 Hz repetition rate with respect to the sequence of steps that

[a]Present address: School of Chemistry, University of Bristol, Cantock's Close, Bristol BS8 1TS, United Kingdom.
[b]Present address: Department of Physics and Astronomy, Vrije Universiteit Amsterdam, De Boelelaan 1081, 1081 HV Amsterdam, Netherlands.
[c]Author to whom correspondence should be addressed: Nick.Walker@newcastle.ac.uk

introduce the chemical sample into the CP-FTMW spectrometer. The solid target rod was continually translated and rotated to ensure that fresh surface material was exposed to each laser pulse. When required to facilitate experiments on isotopically enriched species, samples of each 4-halopyrazole were deuterated at the pyrrolic nitrogen position. The halopyrazole (~2 g) was stirred in THF/D_2O (1:1, 20 mL total) for at least 3 hours before being concentrated to dryness on a rotary evaporator. Further D_2O was added, and this was done for a further 3-4 times with at least one exchange allowed to run overnight. After final concentration, the solid was lyophilised overnight to afford the deuterated product.

The spectrometer and ablation source have been described in detail[23,24] in previous reports describing measurements performed between 7.0 and 18.5 GHz. During the present work, some modifications were made to extend the spectral range to allow the measurement of transitions at frequencies as low as 2.0 GHz. Figure 1 shows a schematic of the current CP-FTMW spectrometer. When measuring spectra between 7.0 and 18.5 GHz, operation is exactly as described previously[23,24] with the exception that the horn antennae have been replaced with larger versions that are effective across a wider frequency range (Steatite Q-Par, QSH-SL-2-18-N-HG-R, 2–18 GHz, 10–22 dBi gain). Various components (highlighted in blue) are removed to allow the measurement of spectra between 2.0 and 8.0 GHz. When performing measurements within this lower frequency range, the chirp produced by the waveform generator is input directly to a traveling-wave tube amplifier (TWTA) that provides amplification in the 2.0–8.0 GHz frequency range (Applied Systems Engineering, Model 167, 450 W). Thus, measurements performed above 8.0 GHz are facilitated by mixing the AWG (arbitrary waveform generator) output [and the free induction decay (FID) of the molecular emission] with the 19.0 GHz output of a phase-locked dielectric resonant oscillator (PDRO), while measurements performed between 2.0 and 8.0 GHz do not require the heterodyne mixing stage.

In order to record a microwave spectrum, molecules within the sample are polarised by a microwave chirp of 1 μs in duration. The free induction decay (FID) of the molecular emission is recorded over the subsequent 20 μs. The gas pulse travels through the interaction region over a longer timeframe so the above sequence of pulses is repeated eight times per gas pulse. FIDs are digitized and recorded by a 100 GS/s digital oscilloscope (Tektronix DPO72304SX) and all data are averaged in the time domain. Fourier transformation is performed using a high resolution window function. Each transition in the frequency domain spectra is observed as a single peak with a full-width at half-maximum of roughly 100 kHz and the estimated precision of frequency measurement is ca. 10 kHz.

III. *AB INITIO* CALCULATIONS

The structures of 4-bromo- and 4-iodopyrazole were optimised using density functional theory (DFT) as implemented in the Gaussian09 software package.[25] The B3LYP functional was used,[26–29] along with the aug-cc-pVTZ basis set for all atoms except iodine.[30–33] In the iodine case, where this basis set was not available, the aug-cc-pVTZ-PP basis set was used with an effective core potential,[34] as obtained from the EMSL basis set exchange.[35,36] Figure 2 shows the results of these calculations, including the orientation of the dipole moments, which have their largest components in the direction of the *b*-axis in both cases (2.19 D for bromopyrazole, 2.18 D for iodopyrazole), with smaller components in the direction of the *a*-axis. Using the geometries obtained as described, the nuclear quadrupole coupling parameters were calculated using DLPNO-CCSD(T)[37] (domain-based, local pair-natural orbitals used within a coupled-cluster method with single, double, and a perturbative treatment of triple excitations) as implemented within the ORCA quantum chemistry package.[38] A QZVP basis set was used throughout and a fine integration grid 7 was adopted for numerical accuracy. Relativistic effects were included using the Douglas Kroll Hess Hamiltonian[39] to the second order and finite nuclear effects[40] were included.

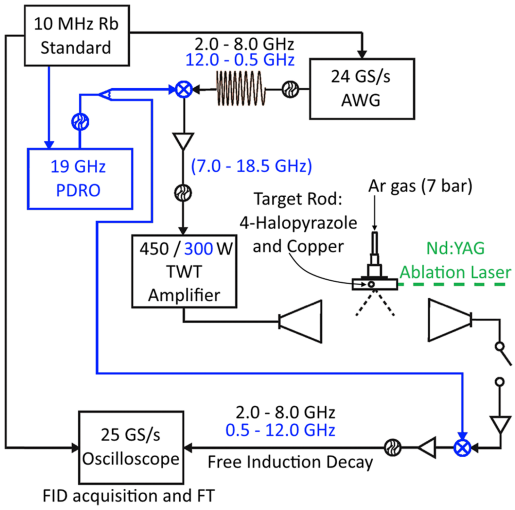

FIG. 1. Schematic diagram of the experimental setup. Components highlighted in blue are included only when operating in the 7.0–18.5 GHz range; when two values for frequency or power are provided, the values in black correspond to operation in the 2.0–8.0 GHz range and the values in blue to operation in the 7.0–18.5 GHz range.

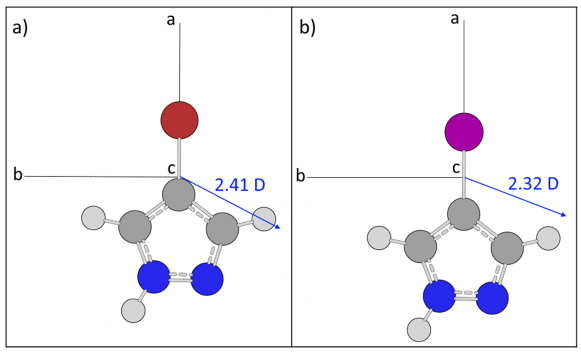

FIG. 2. The structures of (a) 4-bromopyrazole and (b) 4-iodopyrazole as calculated using B3LYP/aug-cc-pVTZ (aug-cc-pVTZ-PP with ECP for iodine) calculations in Gaussian 09. The inertial axes are indicated for each molecule, with the *c*-axis coming out of the page; the centre of mass is at the origin of the axis system. The arrows in blue indicate the orientation and relative magnitude of the dipole moment for each species.

IV. RESULTS

A. Qualitative observations

The spectrum of 4-iodopyrazole was recorded over 220k FIDs in the 2.0–8.0 GHz region and 270k FIDs in the 7.0–18.5 GHz region. The most intense transitions of 4-iodopyrazole were recorded with a signal/noise ratio of 50:1; over one thousand transitions were sufficiently intense to observe. In addition to transitions of 4-iodopyrazole, the observed spectrum displays many peaks that assign to molecules formed by the fragmentation of the precursor. These included $(HCN)_2$,[41,42] CH_3CN,[43] CH_3CCCN,[44,45] HC_3N,[46–48] HC_5N,[49] HC_7N,[50] HC_9N,[51] ICN,[52] ICCCN,[53] $CH_2(CN)_2$,[54,55] cyanoallene,[56,57] and vinyl cyanide (CH_2=CHCN).[58,59] There was evidence of $(H_2O)_2$, which is presumed to be a result of the contamination of the gas lines behind the valve by small amounts of H_2O impurity.[60] Figure 3 shows the spectra recorded in both regions after removal of peaks corresponding to the fragments listed above. Spectra subsequently recorded for the *N*-deuterated isotopologue (510k and 280k FIDs for the 2.0–8.0 GHz and 7.0–18.5 GHz frequency ranges, respectively) revealed transitions of deuterated species including CH_2DCN,[61,62] CHD_2CN,[62,63] CD_3CN,[43] DC_3N,[64] DC_5N,[49] DC_7N,[51] CHD=CHCN,[65] $CHD(CN)_2$,[66] and $CD_2(CN)_2$.[66] Consistent with the relative magnitudes of the *a*- and *b*-components of the dipole moment (calculated to be 0.80 D and 2.18 D, respectively), the observed spectra of both 4-iodopyrazole and its *N*-deuterated isotopologue consist primarily of *b*-type transitions with some *a*-type transitions also observed. The frequency range between 8 and 11 GHz is dominated by Q-branch transitions. Intense R-branch lines are observed at frequencies above the upper limit of this range with weaker R-branch transitions observed throughout the spectrum. An expanded view displaying the hyperfine structure within $J' \rightarrow J''$ transitions of the most intense Q- and R-branches of the parent isotopologue is shown in Fig. 3. Nuclear electric quadrupole coupling interactions between the various quadrupolar nuclei and the electric field gradient at the nucleus introduce significant hyperfine structures into each $J' \rightarrow J''$ transition. Hence, the large intervals between the distinct groups of peaks in the inset of Fig. 3 result from the hyperfine structure introduced by the iodine nucleus (I = 5/2).[67] The smaller splittings apparent within each group result from nuclear quadrupole coupling of the nitrogen nuclei (I = 1).[19,68]

Spectra were measured for the undeuterated isotopologues of 4-bromopyrazole between 2.0–8.0 GHz and 7.0–18.5 GHz and were averaged over 590k and 140k FIDs, respectively. Spectra of the *N*-deuterated isotopologue were recorded over the same frequency ranges and averaged over 200k and 370k FIDs, respectively. Fragmentation products observed in the spectra of 4-bromopyrazole and its N-deuterated isotopologue are generally consistent with the expectation that 4-bromopyrazole disintegrates by similar mechanisms to those followed by 4-iodopyrazole. The most intense transitions of 4-bromopyrazole were observed with a signal/noise ratio of 30:1. The spectra somewhat resemble those of 4-iodopyrazole but are more challenging to assign because bromine has two naturally occurring isotopes (^{79}Br and ^{81}Br) of similar abundance.[69] Approximately 300 transitions were recorded for each of $C_3N_2H_3{}^{79}Br$ and $C_3N_2H_3{}^{81}Br$. Each of the isotopes of bromine possesses a nuclear spin, I = 3/2, and the nuclear quadrupole moments are of similar magnitude.[70] Hyperfine splittings introduced by ^{79}Br and ^{81}Br are therefore similar and responsible for intervals between groups of transitions. These splittings and the isotopic shift are apparent in the inset panes of Fig. 4. The smaller splittings within each individual group of transitions result from nuclear quadrupole coupling of the nitrogen atoms. In similarity with 4-iodopyrazole, the spectrum of 4-bromopyrazole consists primarily of *b*-type transitions that account for between 76% and 85% of assigned features depending on the isotopologue probed. A

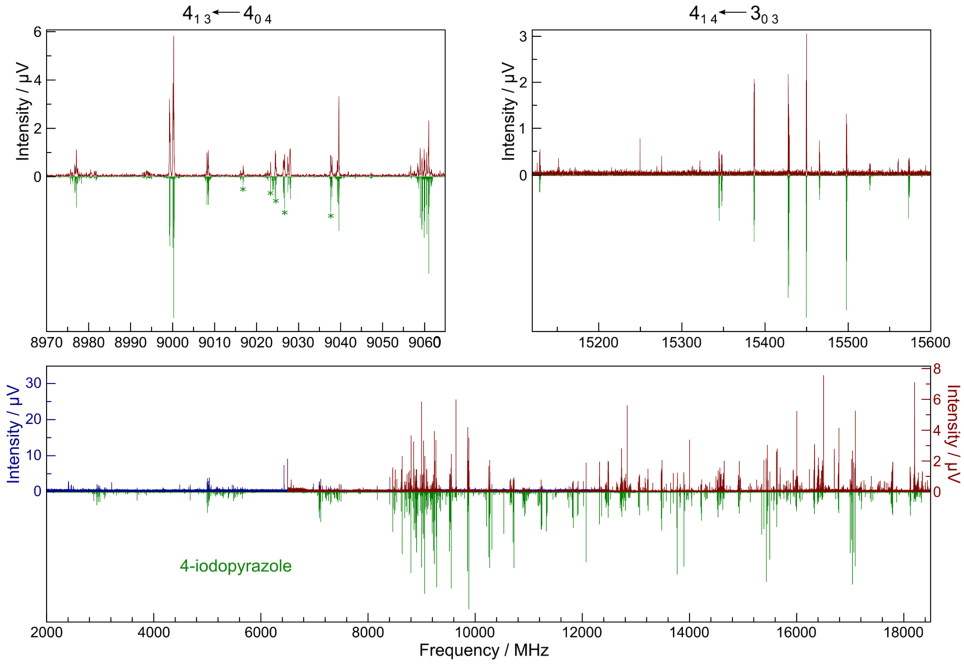

FIG. 3. Microwave spectrum of 4-iodopyrazole recorded in the 2.0–18.5 GHz region. The experimental data are displayed on the top half of each inset. A simulated spectrum generated using PGOPHER (and the constants presented in Table I) is displayed as a negative-going trace. One section from each of a Q- and R-branch is shown in detail (top left and top right insets); starred peaks belong to 4-iodopyrazole transitions that assign to quantum numbers other than those indicated by the inset label.

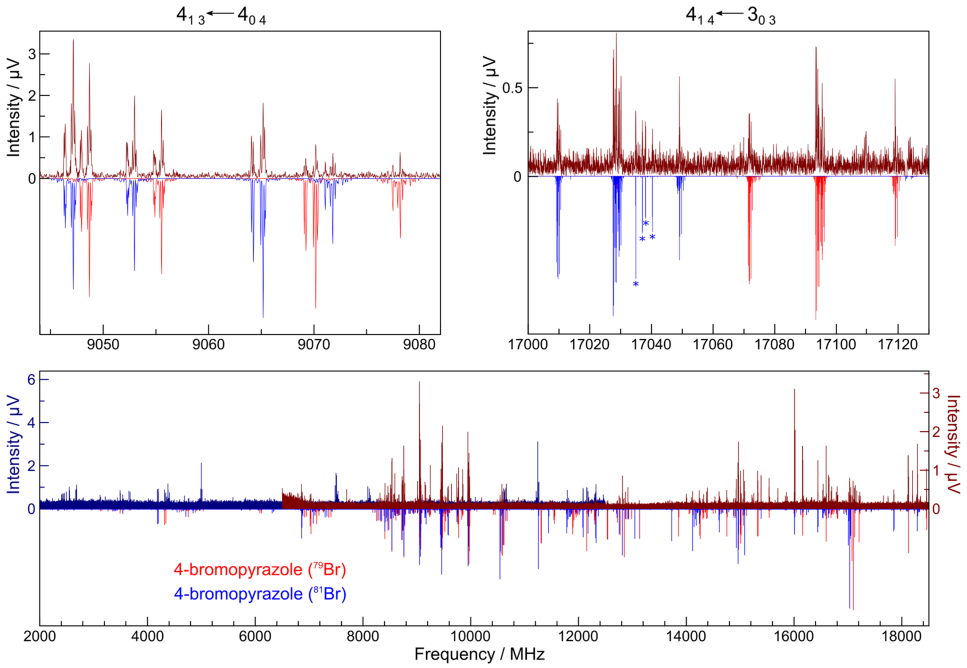

FIG. 4. Microwave spectrum of 4-bromopyrazole recorded in the 2.0–18.5 GHz region. The experimental data are displayed on the top half of each inset. Simulated spectra generated using PGOPHER (and the constants presented in Table II) are displayed as negative-going traces. One section from each of a Q- and R-branch is shown in detail (top left and top right insets); starred peaks belong to 4-bromopyrazole transitions that assign to quantum numbers other than those indicated by the inset label.

strong Q-branch was again observed in the centre of the spectrum between 8 and 11 GHz with R-branch transitions found throughout the range of the spectrum.

B. Determination of spectroscopic constants

Transitions in the spectrum of each halopyrazole were assigned and fitted to determine spectroscopic constants using Western's PGOPHER software package,[71–73] with final fits performed using SPFIT.[74] The Hamiltonian used for each fit was

$$H = H_{\mathrm{R}} - \frac{1}{6}\mathbf{Q}(\mathrm{X}):\boldsymbol{\nabla}\mathbf{E}(\mathrm{X}) - \frac{1}{6}\mathbf{Q}(\mathrm{N1}):\boldsymbol{\nabla}\mathbf{E}(\mathrm{N1}) - \frac{1}{6}\mathbf{Q}(\mathrm{N2}):\boldsymbol{\nabla}\mathbf{E}(\mathrm{N2}), \quad (1)$$

where H_{R} is the energy operator (Watson's A-reduction) for a semi-rigid asymmetric rotor. The remaining terms represent the nuclear electric quadrupole coupling interactions of each quadrupolar nucleus within the molecule with the electric field gradient at that nucleus. The interaction is given by the scalar (or inner) product of the nuclear quadrupole moment dyadic, $\mathbf{Q}$, and the dyadic of the electric field gradient, $\nabla\mathbf{E}$. The halogen atom is represented by X, and the pyrrolic and pyridinic nitrogen atoms are represented by N1 and N2, respectively. The matrix elements of the Hamiltonian were constructed in the coupled asymmetric rotor basis $\boldsymbol{J} + \boldsymbol{I}_1 = \boldsymbol{F}_1$, $\boldsymbol{F}_1 + \boldsymbol{I}_{\mathrm{N1}} = \boldsymbol{F}_2$, $\boldsymbol{F}_2 + \boldsymbol{I}_{\mathrm{N2}} = \boldsymbol{F}$, and diagonalised in blocks of the quantum number, F. Hyperfine structure introduced by the hydrogen and deuterium nuclei was not distinguished at the resolution of the present experiments.

Tables I and II compare the fitted values of rotational, centrifugal distortion, and nuclear quadrupole coupling constants with those calculated *ab initio* for 4-iodopyrazole and 4-bromopyrazole. The agreement between calculated and experimentally determined rotational and centrifugal distortion constants is excellent, confirming that the molecular carriers of the spectra are the described halopyrazoles. Full details of nuclear coordinates in the geometries calculated *ab initio* are provided as supplementary information. The intensities of a- and b-type transitions in all observed spectra are broadly consistent with the expected magnitudes of the dipole moments in these structures. The magnitudes of the experimentally determined nuclear quadrupole coupling constants are less consistent with the theoretical results. An important check of the experimentally determined results involves comparing the nuclear quadrupole coupling constants of isotopologues that are distinct only in respect of the identity of their contained bromine isotope. In these cases, the ratio of nuclear quadrupole coupling constants, $\chi_{aa}(^{79}\mathrm{Br})/\chi_{aa}(^{81}\mathrm{Br})$, is found to be consistent with the ratio of the nuclear quadrupole moments, $Q(^{79}\mathrm{Br})/Q(^{81}\mathrm{Br})$, providing confirmation of the correct line assignments. The calculated $\chi_{aa}(^{79}\mathrm{Br})/\chi_{aa}(^{81}\mathrm{Br})$ ratios are 1.197 094(36) and 1.197 025(43), respectively, for $C_3H_3BrN_2$ and $C_3H_2DBrN_2$, which compare favourably with a benchmark value of 1.197 048(3).[18] Similar agreement is obtained when the equivalent calculation is performed for the experimentally determined values of $\chi_{bb}(\mathrm{Br}) - \chi_{cc}(\mathrm{Br})$.

C. Molecular geometry

4-Iodopyrazole and 4-bromopyrazole are formally asymmetric rotors but very near to the prolate symmetric rotor limit ($\kappa = -0.980$ and -0.964 for $C_3H_3IN_2$ and $C_3H_3BrN_2$, respectively). The level of agreement between the experimentally determined and *ab initio* calculated rotational and centrifugal distortion constants confirms the basic geometry and connectivity of each molecule to be as presented in Fig. 2. The experimentally determined rotational constants allow calculation of an inertial defect, Δ_0, for each halopyrazole,

$$\Delta_0 = I_c^0 - I_a^0 - I_b^0, \quad (2)$$

where I_a^0, I_b^0, and I_c^0 are the moments of inertia determined from the experimentally measured A_0, B_0, and C_0

TABLE I. Spectroscopic constants of 4-iodopyrazole and its *N*-deuterated isotopologue determined experimentally and computationally (numbers in brackets indicate standard deviations in units of last digit).

	$C_3N_2H_3I$		$C_3N_2H_2DI$	
Spectroscopic constant[a]	Expt.[b]	Calc.[c]	Expt.[b]	Calc.[c]
A_0 (MHz)	9495.622 03(88)	9561.143 2	9273.718 42(98)	9335.337 47
B_0 (MHz)	955.218 54(54)	945.109 72	928.986 80(11)	919.152 44
C_0 (MHz)	867.757 62(49)	860.090 60	844.268 72(10)	836.765 00
Δ_J (kHz)	0.033 23(98)	0.032 9	0.030 71(59)	0.030 57
Δ_{JK} (kHz)	0.627 7(91)	0.634	0.605 6(82)	0.587 8
Δ_K (kHz)	2.18(21)	2.71	1.98(25)	2.60
δ_J (Hz)	3.40(11)	3.09	2.998(63)	2.853
δ_K (kHz)	0.82(24)	0.41	...	0.38
χ_{aa} (I) (MHz)	−2007.862 0(93)	−2128.642 3[d]	−2007.767(11)	−2128.593 9[d]
χ_{bb} (I) − χ_{cc} (I) (MHz)	−13.064 0(96)	−43.320 5[d]	−13.134(11)	−43.320 5[d]
$\lvert\chi_{ab}\rvert$ (I) (MHz)	18.96(44)	13.573 4[d]	9.93(74)	13.573[d]
χ_{aa} (N1) (MHz)	0.774(10)	0.781 0[d]	0.759(13)	0.890 8[d]
χ_{bb} (N1) − χ_{cc} (N1) (MHz)	5.356 0(64)	5.507 4[d]	5.354 4(76)	5.739 0[d]
$\lvert\chi_{ab}\rvert$ (N1) (MHz)	0.35(21)	0.215 8[d]	1.13(29)	0.192 3[d]
χ_{aa} (N2) (MHz)	−3.678 7(80)	−4.505 5[d]	−3.654(11)	−4.505 5[d]
χ_{bb} (N2) − χ_{cc} (N2) (MHz)	2.108 8(64)	1.293 7[d]	2.037 6(76)	1.293 7[d]
$\lvert\chi_{ab}\rvert$ (N2) (MHz)	2.14(23)	2.802 7[d]	1.86(22)	2.802 7[d]
N[e]	1120	...	1031	...
$\sigma_{r.m.s.}$ (kHz)[f]	14.1	...	15.1	...

[a]Watson's A reduction.
[b]From SPFIT.
[c]From Gaussian 09 using B3LYP functional and aug-cc-pVTZ basis set (aug-cc-pVTZ-PP with ECP for iodine).
[d]Using DLPNO-CCSD(T) with QZVP-DKH basis set and DKH2 scalar relativistic correction.
[e]Number of transitions included in fit.
[f]Root mean square deviation of fit.

rotational constants. The results for $C_3H_3IN_2$, $C_3H_2DIN_2$, $C_3H_3BrN_2$, and $C_3H_2DBrN_2$ are Δ_0 = 0.1026(6) amu Å^2, 0.0929(1) amu Å^2, 0.0883(1) amu Å^2, and 0.0806(1) amu Å^2, respectively. Such small and positive values are consistent with the expected planar, rigid geometry and are similar to inertial defects established for pyrrole (C_4H_5N) and

TABLE II. Spectroscopic constants of 4-bromopyrazole and its *N*-deuterated isotopologues determined experimentally and computationally (numbers in brackets indicate standard deviations in units of last digit).

	$C_3N_2H_3{}^{79}Br$		$C_3N_2H_2D{}^{79}Br$		$C_3N_2H_3{}^{81}Br$		$C_3N_2H_2D{}^{81}Br$	
Spectroscopic constant[a]	Expt.[b]	Calc.[c]	Expt.[b]	Calc.[c]	Expt.[b]	Calc.[c]	Expt.[b]	Calc.[c]
A_0 (MHz)	9481.054 6(10)	9548.627 8	9261.001 4(10)	9324.3119	9481.048 7(10)	9548.6268	9260.987 5(12)	9324.2986
B_0 (MHz)	1268.296 55(20)	1259.494 63	1232.988 91(20)	1224.39035	1255.611 16(21)	1246.86936	1220.608 31(21)	1212.06957
C_0 (MHz)	1118.433 83(18)	1112.722 91	1087.930 45(19)	1087.27507	1108.556 67(19)	1102.85715	1078.279 20(21)	1072.63702
Δ_J (kHz)	0.048 0(16)	0.051 7	0.044 6(15)	0.0478	0.048 2(17)	0.058	0.042 9(18)	0.0470
Δ_{JK} (kHz)	0.921(31)	0.817	0.792(22)	0.755	0.838(27)	0.805	0.770(24)	0.744
Δ_K (kHz)	2.30(16)	2.49	...	2.38	2.65(13)	2.50	...	2.40
δ_J (Hz)	6.15(26)	6.30	5.09(56)	5.80	6.62(26)	6.14	5.84(27)	5.65
χ_{aa} (Br) (MHz)	590.178(13)	619.005[d]	590.161(13)	550.551	493.009(10)	460.808	493.023(14)	460.845 2
χ_{bb} (Br) − χ_{cc} (Br) (MHz)	−1.977(10)	−5.501[d]	−1.966(12)	−2.991	−1.666(10)	−2.466	−1.641 2(72)	−2.503 5
$\lvert\chi_{ab}\rvert$ (Br) (MHz)	...	8.1[d]	...	2.4	7.3(21)	5.5	6.2(28)	2.0
χ_{aa} (N1) (MHz)	0.786(17)	0.834[d]	0.830(27)	0.830	0.847(18)	0.834	0.832(29)	0.830
χ_{bb} (N1) − χ_{cc} (N1) (MHz)	5.377(10)	5.606[d]	5.446(11)	5.517	5.373 6(96)	5.512	5.419(12)	5.517
χ_{aa} (N2) (MHz)	−3.707(15)	−4.295[d]	−3.613(17)	−3.851	−3.651(14)	−3.908	−3.625(19)	−3.8531
χ_{bb} (N2) − χ_{cc} (N2) (MHz)	2.058(10)	1.222[d]	2.020(11)	1.960	2.076 4(96)	2.015	2.028(12)	1.960 2
N[e]	424	...	290	...	415	...	293	...
$\sigma_{r.m.s.}$ (kHz)[f]	13.1	...	10.8	...	12.9	...	11.7	...

[a]Watson's A reduction.
[b]From SPFIT.
[c]From Gaussian 09 using B3LYP functional and aug-cc-pVTZ basis set.
[d]Using DLPNO-CCSD(T) with QZVP-DKH basis set and DKH2 scalar relativistic correction.
[e]Number of transitions included in fit.
[f]Root mean square deviation of fit.

pyrazole ($C_3H_4N_2$) of 0.016 21(3) amu Å^2 and 0.0316(2) amu Å^2, respectively.[11,75]

Lack of data from a broad range of isotopologues prevents the determination of many bond lengths and angles for either 4-halopyrazole. The coordinates of the hydrogen atom in 4-iodopyrazole, as calculated using Kraitchman's equations,[76] are [−3.8805(4), 1.145(1), 0] Å, in the inertial axis system, where the errors are given by $\delta a = 0.0015/|a|$ Å after Costain[18,77] with the *c*-coordinate fixed at zero. This is consistent with the *ab initio* calculated position of (−3.8787, 1.148, 0) Å, providing further support for assignment to the correct molecular carrier and the accuracy of the calculated molecular structure. The available data allowed the calculation of the *a*, *b*-coordinates of both the hydrogen attached to the pyrrolic hydrogen and the bromine atom in 4-bromopyrazole while fixing the *c*-coordinate to zero in each case. The coordinates of the N-bound hydrogen atom determined by the Kraitchman analysis are [−3.3722(4), 1.144(1), 0] Å compared with (−3.3866, 1.147, 0) Å calculated *ab initio*. The coordinates of the bromine atom determined by the Kraitchman analysis are [1.429(1), 0.0(4), 0] Å compared with (1.436, 0.0, 0) Å from the DFT result. Evidently, the results determined experimentally and those determined by DFT are consistent with respect to these atom coordinates. It should be noted that the substitution coordinates of hydrogen atoms are known to be determined quite poorly by the Kraitchman analysis owing to the significant change in zero-point vibrational energy that accompanies hydrogen/deuterium substitution. The length of the C—Br bond was estimated from the available data by using Kisiel's STRFIT to calculate an r_0 distance.[78] This model involves calculating an r_0 distance from B_0 by the same method as is used to calculate r_e from B_e. It was first necessary to assume that all other bond lengths and angles (those that are internal to the pyrazole sub-unit) are unchanged from those determined by Nygaard *et al.* for the unhalogenated pyrazole monomer.[11] The result of the fit for *r*(C—Br) is 1.8540(12) Å, which is similar to r_0 values of around 1.87 Å found for *r*(C—Br) in other bromine-containing aromatic compounds such as bromobenzene and bromopyridines.[79–81]

D. Nuclear quadrupole coupling constants

Experimental results for nuclear quadrupole coupling constants are conventionally quoted with respect to the inertial axes of the molecule under examination. Comparisons between the nuclear quadrupole coupling constants of a range of molecules will require that all nuclear quadrupole coupling constants are referenced against an appropriate, alternative framework. The various χ_{aa}, χ_{bb}, and χ_{cc} are therefore transformed into the principal nuclear axis system such that a mutually perpendicular set of *x*, *y*, and *z* axes is located on each individual quadrupolar nucleus for comparisons to follow. Both 4-iodopyrazole and 4-bromopyrazole are planar, so each out-of-plane *c*-axis will be parallel to one of the new principal nuclear axes. The *a*- and *b*-axes are transformed onto the remaining axes using the QDIAG program, which is available from the PROSPE database.[82] The angle through which the rotation is performed, ϕ, is determined by the value of χ_{ab} appropriate to the nucleus under examination. $\chi_{ab}(^{79}\text{Br})$ was not determined during the analysis of experimental spectra for $C_3H_3{}^{79}BrN_2$, so the angle of rotation for this isotopologue was assumed to be equal to that determined for $\chi_{ab}(^{81}\text{Br})$ for $C_3H_3{}^{81}BrN_2$. Values were also not determined from χ_{ab} for nitrogen nuclei in 4-bromopyrazole, so the appropriate angles of rotation were determined *ab initio* from the CCSD(T) results for the lighter isotopologue. For each halogen nucleus (denoted by X), the *z*-axis is aligned with the orientation of the C—X bond, and the *y*-axis is perpendicular to the plane of the molecule, with ϕ being the angle between the *a*- and *z*-axes. For the nitrogen nuclei, the convention used by Böttcher *et al.* is adopted,[14] with the *z*-axis perpendicular to the plane and ϕ selected to be the angle between the *a*- and *x*-axes.[14] Table III presents the evaluated components of the nuclear quadrupole coupling tensors of 4-iodopyrazole and 4-bromopyrazole referenced against the appropriate principal nuclear axes. Results are compared with those of the unhalogenated pyrazole molecule.

The nuclear quadrupole coupling constants for the nitrogen atoms in the 4-halopyrazoles studied are very similar to those in unhalogenated pyrazole implying that the electronic environment around the two nitrogen nuclei is not significantly affected by halogenation.[18] Pyrazole is known to attach effectively to enzymes such as ADH,[6,83] and the similarity implies that 4-iodopyrazole and 4-bromopyrazole will retain the capability of pyrazole to form strong hydrogen bonds. The coupling constants for the halogen nuclei can be afforded with more detailed examination due to the simpler environment around these atoms, consisting of a single carbon-halogen bond. The magnitude of the components of the nuclear quadrupole coupling tensors of iodine and bromine provides valuable insight into the possibility that 4-bromo- and 4-iodopyrazole might form halogen bonds.

E. Ionic character and halogen bonding strength

The component of the nuclear quadrupole coupling tensor of the halogen nucleus aligned with the C—X bond, χ_{zz}, can be related to the ionic character of the bond, i_c, by the equation[18]

$$i_c = 1 + \frac{\chi_{zz}}{eQq_{n10}}, \tag{3}$$

where the value of eQq_{n10}, the contribution to the nuclear quadrupole coupling constant from a single *p* electron, is −769.756(16) MHz for ^{79}Br, −643.032(16) MHz for ^{81}Br, and +2292.712(20) MHz for ^{127}I.[18,67,70] The result for each halopyrazole expresses that the fractional ionic character of the C—X bond is equivalent to the partial negative charge on the halogen atom and is displayed in Table IV. The overall trend is toward an increasing partial negative charge on the halogen atom on descending the table.

A halogen bond can be represented in the form M—X···B, where the halogen atom, X, accepts an electron pair from the donor species, B, which is typically an electron-rich species such as a Lewis base.[20] The attraction between these two sub-units depends on the electron distribution around the halogen atom and on the extent of a "σ-hole," an area of low electron density on the halogen atom directly opposite to the R—X bond.[21] Effects that withdraw electron density from the halogen atom, such as the introduction of electronegative substituents on the M group, will tend to increase the depth of the

TABLE III. Nuclear quadrupole coupling constants of pyrazoles in the principal axis system with the angle of rotation from inertial axes (numbers in brackets indicate standard deviations in units of last digit).

Coupling tensor component	4-iodopyrazole $C_3N_2H_3I$	4-bromopyrazole $C_3N_2H_3{}^{79}Br$	4-bromopyrazole $C_3N_2H_3{}^{81}Br$	Pyrazole $C_3N_2H_4$[a]
χ_{zz} (X) (MHz)	−2007.982(11)	590.263(51)	493.081(43)	...
χ_{yy} (X) (MHz)	1010.4630(67)	−294.1006(82)	−245.6717(72)	...
χ_{xx} (X) (MHz)	997.5186(87)	−296.163(50)	−247.410(42)	...
ϕ (X) (deg)	0.3615(84)[b]	0.56(16)[b,c]	0.56(16)	...
χ_{zz} (N1) (MHz)	−3.0650(59)	−3.0814(97)	−3.110(10)	−3.068(9)
χ_{yy} (N1) (MHz)	2.368(88)	2.316	2.286	2.277(29)
χ_{xx} (N1) (MHz)	0.697(89)	0.765	0.824	0.791(36)
ϕ (N1) (deg)	12.4(65)	6.7[d]	7.1[d]	39.74(15)
χ_{zz} (N2) (MHz)	0.7849(51)	0.8245(88)	0.7871(85)	0.853(10)
χ_{yy} (N2) (MHz)	3.53(13)	3.95	3.94	3.621(4)
χ_{xx} (N2) (MHz)	−4.31(13)	−4.78	−4.73	−4.473(10)
ϕ (N2) (deg)	16.5(14)	20.5[d]	20.7[d]	14.35(4)

[a]Reference 14.
[b]The implied rotation places the halogen atom and the pyrrolic nitrogen atom on opposite sides of the *a*-inertial axis.
[c]Fixed at values obtained for ^{81}Br isotopologue.
[d]Using the *ab initio* χ_{ab} value from CCSD(T) calculations performed on the isotopologue containing ^{79}Br ($|\chi_{ab}|$ = 0.179 MHz for N1, 2.866 MHz for N2).

σ-hole and thus the strength of the halogen bond.[84–86] Table IV compares values of χ_{zz} and i_c for 4-halopyrazoles with those for other brominated or iodinated aromatic molecules for which microwave spectroscopy data are available and the reference species, CH_3X, CF_3X, and XCl. The molecules included in Table IV are ranked in the order of decreasing χ_{zz}(Br) although the ordering is broadly similar if molecules are ranked in the order of decreasing χ_{zz}(I).

TABLE IV. Components of nuclear quadrupole coupling tensors aligned with the C—X bond, χ_{zz}, and ionic character of the associated bond, i_c, for bromine- and iodine-containing molecules.

Compound	Bromo- χ_{zz} (^{79}Br) (MHz)	Bromo- i_c	Iodo- χ_{zz} (^{127}I) (MHz)	Iodo- i_c
XCl[a]	875.309(1)	−0.361	−2928.821(4)	−0.277
CF_3X[b]	618.2628(21)	0.197	−2144.9949(28)	0.064
2-halothiophene[c]	599.8(22)	0.221	−2058.5(22)	0.102
2-halopyrimidine[d]	597.8(7)	0.223	...	...
4-halopyrazole[e]	590.263(51)	0.233	−2007.982(11)	0.124
CH_3X[f]	577.1343(31)	0.250	−1934.080(10)	0.156
3-halothiophene[g]	574.97(9)	0.253	−1994.6(16)	0.130
3-halopyridine[h]	561.3(29)	0.271	−1932.338(67)	0.157
4-halopyridine[i]	557.3(13)	0.276	−1938(2)	0.155
Halobenzene[j]	556.6783(17)	0.277	−1892.0398(46)	0.175
p-halotoluene[k]	555.618(8)	0.278	−1886.202(12)	0.177
2-halopyridine[i]	555.2(12)	0.283	−1881(2)	0.180

[a]References 88 and 89.
[b]References 90 and 23.
[c]References 91–93.
[d]Reference 94.
[e]This work.
[f]References 95 and 96.
[g]References 97 and 98.
[h]References 80 and 99.
[i]References 79 and 100.
[j]References 101 and 102.
[k]Reference 103.

The relative strengths of the halogen bonds formed by each of CF_3I and ICl (where the halogen bond is formed with the iodine atom) were discussed within a previous study.[87] The comparison was between the values of k_σ, the force constant of the halogen bond formed between the iodine atom and the Lewis base, B, in the B···ICl and B···ICF_3 series (where B is Kr, CO, H_2S, or NH_3), which was calculated from centrifugal distortion constants determined by rotational spectroscopy. It was shown that the magnitude of k_σ in B···ICF_3 is consistently a factor of two smaller than that in B···ICl for a given B. For example, the values of k_σ in OC···ICF_3 and OC···ICl are, respectively, 3.95 and 8.0 N m^{-1} while those in H_3N···ICF_3 and H_3N···ICl are, respectively, 11.6(2) and 30.4 N m^{-1}. The value of χ_{zz}(I) for the CF_3I monomer is −2144.9949(28) while that for ICl is −2928.821(4) MHz. Evidently, with respect to a comparison between CF_3I and ICl, there is a broad correlation between the magnitude of χ_{aa}(I) and the strengths of the halogen bonds formed by these species. This is unsurprising because a larger value of χ_{zz} implies a smaller negative charge on the halogen atom and thus a larger "σ-hole."

It can be seen from Table IV that the 4-halopyrazole compounds have values of χ_{zz}(X) that are intermediate between those of CH_3X and CF_3X, which implies that the 4-halopyrazoles may form halogen bonds of similar strength to those formed by these comparators. However, it is important to note that small variations of χ_{zz}(X) along the series shown in Table IV do not necessarily indicate an identical trend in respect of the strengths of the halogen bonds formed by these molecules. Zero-point effects will be different for each molecule, the electric field gradient at the nucleus [which can be calculated from χ_{zz}(X)] will not ideally represent the electron density within bonding molecular orbitals, and the incremental variations of χ_{zz}(X) displayed in Table IV are much smaller than the large difference between the respective values of χ_{zz}(X) for CF_3I and ICl.

Bauman *et al.* explored the tendency of a range of molecules to bind to the protein HIV-1 reverse transcriptase (RT).[7] The range studied included 2-bromopyrimidine, 4-bromopyridine, 4-iodopyridine, and 2-bromopyridine, for which various data are provided in Table IV. While 2-bromopyrimidine was found to bind to 4 protein sites, the remaining three molecules were not observed to attach to the protein.[7] Broadly correlating the magnitude of χ_{aa}(I) with the strength of halogen bonds formed by each molecule, 2-bromopyrimidine has a very high value of χ_{zz}(Br), which is comparable with that of 4-bromopyrazole implying that 2-bromopyrimidine may form reasonably strong halogen bonds. Given that halogen bonds are highly directional such that M—X···B tends to linearity, the formation of a halogen bond between 2-bromopyrimidine (or any of the other molecules listed above) and RT would require a favourable interaction geometry. It is possible that the high binding tendency of 2-bromopyrimidine also relates to an ability to form hydrogen bonds. However, the nitrogen atoms in 2-bromopyrimidine are adjacent to the bromine atom and therefore perhaps less optimally positioned for the formation of hydrogen bonds than those in 4-bromo- and 4-iodopyridine.

Bauman *et al.* noted that 4-bromo- and 4-iodopyrazole are able to attach to 15 and 21 binding sites on RT, respectively, significantly more than any other species examined.[7] From the data obtained during this work, a partial explanation of this high binding tendency can be provided. The implication of the present work is that 4-halopyrazoles are likely to form halogen bonds that are broadly comparable in strength to those formed by CH_3X and CF_3X. Measurements of the nuclear quadrupole coupling constants of the nitrogen atoms within the halopyrazoles confirm that charge distribution around the pyrazole sub-unit is not significantly perturbed by the presence of the halogen atom. This implies that the halopyrazoles will retain the strong hydrogen bonding ability of the (unhalogenated) pyrazole monomer. The hydrogen and halogen bonding sites in the 4-halopyrazoles are located on opposite sides of the pyrazole ring. Consequently, stable bridging binding modes involving hydrogen and/or halogen bonds can be envisaged between different protein sites, as observed by Bauman *et al.*,[7] while the small size of the molecule (being only a five-membered ring) will assist access to binding pockets. The fact that 4-iodopyrazole tends to bind to a greater number of binding sites than 4-bromopyrazole is unsurprising because the more polarisable iodine atom is able to form deeper σ-holes and thus stronger halogen bonds.[21]

V. CONCLUSIONS

The pure rotational spectra of 4-bromo- and 4-iodopyrazole have been recorded in the 2.0–18.5 GHz region. Rotational, centrifugal distortion and nuclear quadrupole coupling constants appropriate to the vibrational ground state of each molecule have been precisely determined from the experimentally observed spectra. Geometrical parameters determined from the rotational constants are consistent with molecular geometries calculated using density functional theory. The measured nuclear quadrupole coupling constants have been analyzed to explore the distribution of charge within these molecules. The data confirm that both 4-bromo- and 4-iodopyrazole may form halogen bonds and will retain the ability of pyrazole to form hydrogen bonds to proteins. The rotational spectra of molecules in excited vibrational states have been previously measured by the technique employed here. While over a thousand transitions were assigned during the present work, the number of transitions recorded but not assigned to a molecular carrier was very small. It is therefore not possible to confirm whether the methods employed herein might allow the generation and study of rotational spectra of vibrationally excited states of either 4-iodopyrazole or 4-bromopyrazole.

SUPPLEMENTARY MATERIAL

See supplementary material for (i) lists of observed transition frequencies and quantum number assignments for each isotopologue investigated and (ii) *ab initio* calculated coordinates of nuclei in 4-bromopyrazole and 4-iodopyrazole.

ACKNOWLEDGMENTS

The authors thank the European Research Council for the postdoctoral fellowships awarded to G.A.C. and C.M. and for project funding (Grant No. CPFTMW-307000). We are grateful to Professor Anthony C. Legon for a critical reading of the manuscript, to Professor Mike Waring of Newcastle University for alerting us to the importance of halopyrazoles in biochemical structure determination, to Dr. Alistair Henderson of NewChem Technologies for preparation of the deuterated samples, and to Newcastle University for the award of a Research Excellence Academy studentship to J.D.L.

[1] F. K. Keter and J. Darkwa, BioMetals **25**(1), 9–21 (2012).
[2] L. Goldberg and U. Rydberg, Biochem. Pharmacol. **18**(7), 1749–1762 (1969).
[3] J. Brent, K. McMartin, S. Phillips, C. Aaron, and K. Kulig, N. Engl. J. Med. **344**(6), 424–429 (2001).
[4] D. G. Barceloux, G. R. Bond, E. P. Krenzelok, H. Cooper, and J. A. Vale, J. Toxicol.: Clin. Toxicol. **40**(4), 415–446 (2002).
[5] U. S. Rydberg, Biochem. Pharmacol. **18**(10), 2425–2428 (1969).
[6] T.-K. Li and H. Theorell, Acta Chem. Scand. **23**, 892–902 (1969).
[7] J. D. Bauman, J. J. E. K. Harrison, and E. Arnold, IUCrJ **3**(1), 51–60 (2016).
[8] W. H. Kirchhoff, J. Am. Chem. Soc. **89**(6), 1312–1316 (1967).
[9] G. L. Blackman, R. D. Brown, and F. R. Burden, J. Mol. Spectrosc. **36**(3), 528–540 (1970).
[10] G. L. Blackman, R. D. Brown, F. R. Burden, and A. Mishra, J. Mol. Struct. **9**(4), 465–473 (1971).
[11] L. Nygaard, D. Christen, J. T. Nielsen, E. J. Pedersen, O. Snerling, E. Vestergaard, and G. O. Sørensen, J. Mol. Struct. **22**(3), 401–413 (1974).
[12] R. S. Nasibullin, R. G. Latypova, V. S. Troitskaya, V. G. Vinokurov, and N. M. Pozdeev, J. Struct. Chem. **15**(1), 41–44 (1974).
[13] M. Stolze and D. H. Sutter, Z. Naturforsch., A: Phys. Sci. **42**(1), 49–56 (1987).
[14] O. Böttcher and D. H. Sutter, Z. Naturforsch., A: Phys. Sci. **45**(11-12), 1248–1258 (1990).
[15] S. Blanco, J. C. López, J. Alonso, O. Mó, M. Yáñez, N. Jagerovic, and J. Elguero, J. Mol. Struct. **344**(3), 241–250 (1995).
[16] J. Limtrakul, Monatsh. Chem. Chem. Mon. **124**(3), 259–266 (1993).
[17] W. Caminati, P. G. Favero, and B. Velino, Chem. Phys. **239**(1–3), 223–227 (1998).
[18] W. Gordy and R. L. Cook, *Microwave Molecular Spectra*, 3rd ed. (John Wiley & Sons, New York, 1984).

[19]S. E. Novick, J. Mol. Spectrosc. **267**(1–2), 13–18 (2011).
[20]P. Politzer, P. Lane, M. C. Concha, Y. Ma, and J. S. Murray, J. Mol. Model. **13**(2), 305–311 (2007).
[21]T. Clark, M. Hennemann, J. S. Murray, and P. Politzer, J. Mol. Model. **13**(2), 291–296 (2007).
[22]J. G. Hill, A. C. Legon, D. P. Tew, and N. R. Walker, in *Halogen Bonding I: Impact on Materials Chemistry and Life Sciences*, edited by P. Metrangolo and G. Resnati (Springer International Publishing, Cham, 2015), pp. 43–77.
[23]S. L. Stephens and N. R. Walker, J. Mol. Spectrosc. **263**(1), 27–33 (2010).
[24]D. P. Zaleski, S. L. Stephens, and N. R. Walker, Phys. Chem. Chem. Phys. **16**(46), 25221–25228 (2014).
[25]M. J. Frisch, G. W. Trucks, H. B. Schlegel, G. E. Scuseria, M. A. Robb, J. R. Cheeseman, G. Scalmani, V. Barone, B. Mennucci, G. A. Petersson, H. Nakatsuji, M. Caricato, X. Li, H. P. Hratchian, A. F. Izmaylov, J. Bloino, G. Zheng, J. L. Sonnenberg, M. Hada, M. Ehara, K. Toyota, R. Fukuda, J. Hasegawa, M. Ishida, T. Nakajima, Y. Honda, O. Kitao, H. Nakai, T. Vreven, J. A. Montgomery, Jr., J. E. Peralta, F. Ogliaro, M. Bearpark, J. J. Heyd, E. Brothers, K. N. Kudin, V. N. Staroverov, T. Keith, R. Kobayashi, J. Normand, K. Raghavachari, A. Rendell, J. C. Burant, S. S. Iyengar, J. Tomasi, M. Cossi, N. Rega, J. M. Millam, M. Klene, J. E. Knox, J. B. Cross, V. Bakken, C. Adamo, J. Jaramillo, R. Gomperts, R. E. Stratmann, O. Yazyev, A. J. Austin, R. Cammi, C. Pomelli, J. W. Ochterski, R. L. Martin, K. Morokuma, V. G. Zakrzewski, G. A. Voth, P. Salvador, J. J. Dannenberg, S. Dapprich, A. D. Daniels, O. Farkas, J. B. Foresman, J. V. Ortiz, J. Cioslowski, and D. J. Fox, GAUSSIAN 09, Revision D.01, Gaussian, Inc., Wallingford, CT, 2013.
[26]A. D. Becke, J. Chem. Phys. **98**(7), 5648–5652 (1993).
[27]C. Lee, W. Yang, and R. G. Parr, Phys. Rev. B **37**(2), 785–789 (1988).
[28]B. Miehlich, A. Savin, H. Stoll, and H. Preuss, Chem. Phys. Lett. **157**(3), 200–206 (1989).
[29]S. H. Vosko, L. Wilk, and M. Nusair, Can. J. Phys. **58**(8), 1200–1211 (1980).
[30]T. H. Dunning, Jr., J. Chem. Phys. **90**(2), 1007–1023 (1989).
[31]A. K. Wilson, D. E. Woon, K. A. Peterson, and T. H. Dunning, Jr., J. Chem. Phys. **110**(16), 7667–7676 (1999).
[32]R. A. Kendall, T. H. Dunning, Jr., and R. J. Harrison, J. Chem. Phys. **96**(9), 6796–6806 (1992).
[33]E. R. Davidson, Chem. Phys. Lett. **260**(3), 514–518 (1996).
[34]K. A. Peterson, B. C. Shepler, D. Figgen, and H. Stoll, J. Phys. Chem. A **110**(51), 13877–13883 (2006).
[35]D. Feller, J. Comput. Chem. **17**(13), 1571–1586 (1996).
[36]K. L. Schuchardt, B. T. Didier, T. Elsethagen, L. Sun, V. Gurumoorthi, J. Chase, J. Li, and T. L. Windus, J. Chem. Inf. Model. **47**(3), 1045–1052 (2007).
[37]M. Sparta and F. Neese, Chem. Soc. Rev. **43**(14), 5032–5041 (2014).
[38]F. Neese, Wiley Interdiscip. Rev.: Comput. Mol. Sci. **2**(1), 73–78 (2012).
[39]M. Reiher and A. Wolf, J. Chem. Phys. **121**(22), 10945–10956 (2004).
[40]L. Visscher and K. G. Dyall, At. Data Nucl. Data Tables **67**(2), 207–224 (1997).
[41]A. C. Legon, D. J. Millen, and P. J. Mjöberg, Chem. Phys. Lett. **47**(3), 589–591 (1977).
[42]R. E. Bumgarner and G. A. Blake, Chem. Phys. Lett. **161**(4-5), 308–314 (1989).
[43]M. Kessler, H. Ring, R. Trambarulo, and W. Gordy, Phys. Rev. **79**(1), 54–56 (1950).
[44]J. Sheridan and L. F. Thomas, Nature **174**(4434), 798 (1954).
[45]M. Bester, M. Tanimoto, B. Vowinkel, G. Winnewisser, and K. Yamada, Z. Naturforsch., A: Phys. Sci. **38**(1), 64 (1983).
[46]A. A. Westenberg and E. B. Wilson, Jr., J. Am. Chem. Soc. **72**(1), 199–200 (1950).
[47]R. L. de Zafra, Astrophys. J. **170**, 165–168 (1971).
[48]S. Thorwirth, H. S. P. Müller, and G. Winnewisser, J. Mol. Spectrosc. **204**(1), 133–144 (2000).
[49]A. J. Alexander, H. W. Kroto, and D. R. M. Walton, J. Mol. Spectrosc. **62**(2), 175–180 (1976).
[50]C. Kirby, H. W. Kroto, and D. R. M. Walton, J. Mol. Spectrosc. **83**(2), 261–265 (1980).
[51]M. C. McCarthy, E. S. Levine, A. J. Apponi, and P. Thaddeus, J. Mol. Spectrosc. **203**(1), 75–81 (2000).
[52]J. Gripp, H. Dreizler, J. Gadhi, G. Wlodarczak, J. Legrand, J. Burie, and J. Demaison, J. Mol. Spectrosc. **129**(2), 381–387 (1988).
[53]T. Bjorvatten, J. Mol. Struct. **20**(1), 75–82 (1974).
[54]J. Burie, D. Boucher, J. Demaison, and A. Dubrulle, J. Phys. **43**(9), 1319–1325 (1982).
[55]A. P. Cox, Y. Kawashima, E. Fliege, and H. Dreizler, Z. Naturforsch. A **40**(4), 361–367 (1985).
[56]A. Bouchy, J. Demaison, G. Roussy, and J. Barriol, J. Mol. Struct. **18**(2), 211–217 (1973).
[57]G. Schwahn, R. Schieder, M. Bester, and G. Winnewisser, J. Mol. Spectrosc. **116**(2), 263–270 (1986).
[58]W. S. Wilcox, J. H. Goldstein, and J. W. Simmons, J. Chem. Phys. **22**(3), 516–518 (1954).
[59]J. Demaison, J. Cosleou, R. Bocquet, and A. G. Lesarri, J. Mol. Spectrosc. **167**(2), 400–418 (1994).
[60]L. H. Coudert and J. T. Hougen, J. Mol. Spectrosc. **139**(2), 259–277 (1990).
[61]H. S. P. Müller, B. J. Drouin, and J. C. Pearson, Astron. Astrophys. **506**(3), 1487–1499 (2009).
[62]L. Nguyen, A. Walters, L. Margulès, R. A. Motiyenko, J. C. Guillemin, C. Kahane, and C. Ceccarelli, Astron. Astrophys. **553**, A84 (2013).
[63]L. Halonen and I. M. Mills, J. Mol. Spectrosc. **73**(3), 494–502 (1978).
[64]H. Spahn, H. S. P. Müller, T. F. Giesen, J.-U. Grabow, M. E. Harding, J. Gauss, and S. Schlemmer, Chem. Phys. **346**(1-3), 132–138 (2008).
[65]J. M. Colmont, G. Wlodarczak, D. Priem, H. S. P. Müller, E. H. Tien, R. J. Richards, and M. C. L. Gerry, J. Mol. Spectrosc. **181**(2), 330–344 (1997).
[66]J. Randell, A. P. Cox, I. Merke, and H. Dreizler, J. Chem. Soc., Faraday Trans. **86**(11), 1981–1989 (1990).
[67]V. Jaccarino, J. G. King, R. A. Satten, and H. H. Stroke, Phys. Rev. **94**(6), 1798–1799 (1954).
[68]A. Schirmacher and H. Winter, Phys. Rev. A **47**(6), 4891–4907 (1993).
[69]J. R. de Laeter, J. K. Böhlke, P. de Bièvre, H. Hidaka, H. S. Peiser, K. J. R. Rosman, and P. D. P. Taylor, Pure Appl. Chem. **75**(6), 683–800 (2003).
[70]J. G. King and V. Jaccarino, Phys. Rev. **94**(6), 1610–1616 (1954).
[71]C. M. Western, J. Quant. Spectrosc. Radiat. Transfer **186**, 221–242 (2017).
[72]C. M. Western, PGOPHER, A Program for Simulating Rotational, Vibrational and Electronic Spectra, University of Bristol, http://pgopher.chm.bris.ac.uk.
[73]C. M. Western, PGOPHER version 9.1, University of Bristol Research Data Repository, 2016.
[74]H. M. Pickett, J. Mol. Spectrosc. **148**(2), 371–377 (1991).
[75]G. Wlodarczak, L. Martinache, J. Demaison, and B. P. van Eijck, J. Mol. Spectrosc. **127**(1), 200–208 (1988).
[76]J. Kraitchman, Am. J. Phys. **21**(1), 17–24 (1953).
[77]C. C. Costain, Trans. Am. Crystallogr. Assoc. **2**, 157–164 (1966).
[78]Z. Kisiel, J. Mol. Spectrosc. **218**(1), 58–67 (2003).
[79]W. Caminati and P. Forti, Chem. Phys. Lett. **15**(3), 343–349 (1972).
[80]S. Doraiswamy and S. D. Sharma, J. Mol. Spectrosc. **88**(1), 95–108 (1981).
[81]S. A. Peebles and R. A. Peebles, J. Mol. Struct. **657**(1-3), 107–116 (2003).
[82]Z. Kisiel, in *Spectroscopy from Space*, edited by J. Demaison, K. Sarka, and E. A. Cohen (Kluwer Academic Publishers, Dordrecht, 2001), pp. 91–106.
[83]H. Theorell, T. Yonetani, and B. Sjöberg, Acta Chem. Scand. **23**, 255–260 (1969).
[84]K. E. Riley, J. S. Murray, J. Fanfrlík, J. Řezáč, R. J. Solá, M. C. Concha, F. M. Ramos, and P. Politzer, J. Mol. Model. **17**(12), 3309–3318 (2011).
[85]K. E. Riley, J. S. Murray, J. Fanfrlík, J. Řezáč, R. J. Solá, M. C. Concha, F. M. Ramos, and P. Politzer, J. Mol. Model. **19**(11), 4651–4659 (2013).
[86]R. Wilcken, M. O. Zimmermann, A. Lange, A. C. Joerger, and F. M. Boeckler, J. Med. Chem. **56**(4), 1363–1388 (2013).
[87]S. L. Stephens, N. R. Walker, and A. C. Legon, J. Chem. Phys. **135**(22), 224309 (2011).
[88]J. B. Davey, A. C. Legon, and E. R. Waclawik, Chem. Phys. Lett. **306**(3-4), 133–144 (1999).
[89]A. C. Legon and J. C. Thorn, Chem. Phys. Lett. **215**(6), 554–560 (1993).
[90]A. J. Gray and R. J. Butcher, J. Mol. Spectrosc. **161**(2), 351–368 (1993).
[91]P. J. Mjöberg, W. M. Ralowski, and S. O. Ljunggren, Z. Naturforsch., A: Phys. Sci. **30**(4), 541–548 (1975).
[92]P. J. Mjöberg, W. M. Ralowski, and S. O. Ljunggren, Z. Naturforsch., A: Phys. Sci. **30**(10), 1332 (1975).
[93]Y. Niide, I. Ohkoshi, and Y. Sasada, J. Mol. Spectrosc. **128**(2), 580–586 (1988).
[94]J. Chen, C. D. Paulse, and R. W. Davis, J. Mol. Spectrosc. **145**(1), 18–28 (1991).
[95]M. Ramos and B. J. Drouin, J. Mol. Spectrosc. **269**(2), 187–192 (2011).

[96]G. Wlodarczak, D. Boucher, R. Bocquet, and J. Demaison, J. Mol. Spectrosc. **124**(1), 53–65 (1987).
[97]D. Hübner, E. Fliege and D. H. Sutter, Z. Naturforsch., A: Phys. Sci. **38**(11), 1238–1247 (1983).
[98]Y. Niide and I. Ohkoshi, J. Mol. Spectrosc. **130**(1), 230–237 (1988).
[99]S. A. Gaster, G. G. Brown, S. Arnold, and T. M. Hall, in *Presented at the 70th International Symposium on Molecular Spectroscopy* (University of Illinois at Urbana-Champaign, USA, 2015).
[100]W. Caminati and P. Forti, Chem. Phys. Lett. **29**(2), 239–241 (1974).
[101]O. Dorosh, E. Białkowska-Jaworska, Z. Kisiel, and L. Pszczółkowski, J. Mol. Spectrosc. **246**(2), 228–232 (2007).
[102]J. L. Neill, S. T. Shipman, L. Alvarez-Valtierra, A. Lesarri, Z. Kisiel, and B. H. Pate, J. Mol. Spectrosc. **269**(1), 21–29 (2011).
[103]V. A. Shubert, D. Schmitz, and M. Schnell, Mol. Phys. **111**(14-15), 2189–2197 (2013).